

Fatty Acids can Substitute the HIV Fusion Peptide in Lipid Merging and Fusion: An Analogy between Viral and Palmitoylated Eukaryotic Fusion Proteins

Naama Lev and Yechiel Shai*

Department of Biological
Chemistry, The Weizmann
Institute of Science, Rehovot
76100 Israel

Received 10 June 2007;
received in revised form
20 August 2007;
accepted 4 September 2007
Available online
11 September 2007

Various fusion proteins from eukaryotes and viruses share structural similarities such as a coiled coil motif. However, compared with eukaryotic proteins, a viral fusion protein contains a fusion peptide (FP), which is an N-terminal hydrophobic fragment that is primarily involved in directing fusion via anchoring the protein to the target cell membrane. In various eukaryotic fusion proteins the membrane targeting domain is cysteine-rich and must undergo palmitoylation prior to the fusion process. Here we examined whether fatty acids can replace the FP of human immunodeficiency virus type 1 (HIV-1), thereby discerning between the contributions of the sequence *versus* hydrophobicity of the FP in the lipid-merging process. For that purpose, we structurally and functionally characterized peptides derived from the N terminus of HIV fusion protein - gp41 in which the FP is lacking or replaced by fatty acids. We found that fatty acid conjugation dramatically enhanced the capability of the peptides to induce lipid mixing and aggregation of zwitterionic phospholipids composing the outer leaflet of eukaryotic cell membranes. The enhanced effect of the acylated peptides on membranes was further supported by real-time atomic force microscopy (AFM) showing nanoscale holes in zwitterionic membranes. Membrane-binding experiments revealed that fatty acid conjugation did not increase the affinity of the peptides to the membrane significantly. Furthermore, all free and acylated peptides exhibited similar α -helical structures in solution and in zwitterionic membranes. Interestingly, the fusogenic active conformation of N36 in negatively charged membranes composing the inner leaflet of eukaryotic cells is β -sheet. Apparently, N-terminal heptad repeat (NHR) can change its conformation as a response to a change in the charge of the membrane head group. Overall, the data suggest an analogy between the eukaryotic cysteine-rich domains and the viral fusion peptide, and mark the hydrophobic nature of FP as an important characteristic for its role in lipid merging.

© 2007 Elsevier Ltd. All rights reserved.

Edited by J. Karn

Keywords: membrane fusion; peptide–lipid interaction; HIV-1 gp41; AFM; fusion peptide

*Corresponding author. E-mail address:
Yechiel.Shai@weizmann.ac.il.

Abbreviations used: FP, fusion peptide; HIV-1, human immunodeficiency virus type 1; AFM, atomic force microscopy; NHR, N-terminal heptad repeat; CHR, C-terminal heptad repeat; SHB, six helix bundle; LUV, large unilamellar vesicles; SUV, unilamellar vesicles; ATR, attenuated total reflection; FTIR, fourier transform infrared; PC, phosphatidyl choline; PS, phosphatidyl serine

Introduction

Human immunodeficiency virus (HIV), like other enveloped viruses, employs fusion proteins in order to enter and infect target cells. The HIV fusion protein is the glycoprotein gp41, a transmembrane protein that is linked non-covalently to the surface glycoprotein gp120. Together, gp120 and gp41 form the enveloped (ENV) glycoprotein complex^{1,2} that is embedded in the viral membrane as a trimmer.³

gp41, like other types of transmembrane proteins, is composed of cytoplasmic, transmembrane, and extracellular domains. The extracellular domain (ectodomain) contains four major functional regions: closest to the viral membrane is a Trp-rich pretransmembrane domain (PTD), followed by a C-terminal heptad repeat (CHR), an N-terminal heptad repeat (NHR), and a stretch of 15 hydrophobic residues, located in the N terminus, termed fusion peptide (FP).⁴

Prior to fusion, gp41 is held in a metastable state by gp120. Fusion is initiated by specific binding of gp120 to the CD4 cell surface receptor,⁵ which induces major conformational changes in gp120, thereby changing gp41 metastable constraints, resulting in its activation.^{2,6} FP inserts into the target membrane⁷ and gp41 adopts a trimeric extended pre-hairpin intermediate (PHI) conformation that connects both viral and cellular membranes.^{8,9} The original model suggests that the PHI conformation, which is characterized by exposed NHR and CHR regions, is short lived and collapses after up to 30 min into a low-energy conformation of six helix bundle (SHB).^{10,11} In the SHB conformation, the α -helical CHR regions are packed into hydrophobic grooves on the surface of the NHR coiled coil in an antiparallel manner.^{12,13} Although SHB conformation is believed to pool together viral and cell membranes, a step required for fusion, it has been recently shown that the fusion pores are formed before the folding into the SHB conformation is complete.¹⁴ Identification of the sequential events that take place following gp41 activation, leading to pore formation, have been studied intensively; however, the exact role of gp41 in the mechanism of fusion is yet to be elucidated.

The FP plays a central role in the viral fusion, since single amino acid mutations in this region lead to reduced fusogenic activity of gp41-derived peptides, as well as to decreased virus infectivity.¹⁵⁻¹⁹ After gp41 is released from its metastable constraints, FP is believed to insert into the target membrane, providing a hydrophobic anchor,²⁰ consequently perturbing the target membrane. Such an equivalent hydrophobic fusion peptide does not exist in various fusion proteins that participate in compartmentalization in eukaryotic cells.²¹ Instead, they have a highly conserved cysteine-rich domain that plays an important role in membrane targeting. These cysteine-rich domains are not intrinsically hydrophobic,²²; however, the attachment of palmitic acid to the cysteine residue adds additional hydrophobicity to the region.²³ For example, synaptosome-associated proteins SNAP 23/25 are fusion proteins participating in exocytosis in mammal cells. It was shown that palmitoylation is necessary for their function in the fusion process, since it is essential for membrane association.²²

In the case of HIV-1, in addition to FP, essential for anchoring gp41 to the target membrane²⁰ and perturbing it, other regions of gp41 were also shown to be involved in membrane destabilization and fusion of viral and host membranes.^{1,24-33}

Moreover, FP and NHR regions act synergistically in the actual fusion process when conjugated together, suggesting that FP facilitates peptide partition into the target membrane, whereas NHR assists in the membrane fusion event.²⁸ Similar results were obtained for the influenza and sendai fusogenic domains.^{34,35} Interestingly, the fusion peptide varies considerably among different viral strains but its hydrophobic nature is preserved.³⁶ However, it is yet not clear whether the specific amino acid sequence is important for its function in the actual membrane fusion process or for its remarkable hydrophobicity.

Collectively, it appears that the hydrophobic viral FP and palmitoylation in various eukaryotic fusion proteins are playing an analogous role in the actual fusion process. In light of this assumption, we have studied here the effect of substituting FP for fatty acids on the structure and function of HIV gp41-derived peptides. Two different N-terminal gp41 fragments were synthesized. One comprises the NHR (N36) and the second comprises the NHR and the adjacent polar region (N54). Palmitic or decanoic acids were coupled to the different peptides. The GCN4 coiled-coil conjugated to fatty acids served as a negative control. All constructs were functionally characterized for their ability to induce aggregation/fusion and lipid mixing of phosphatidyl choline (PC) large unilamellar vesicles (LUV), their effect on the morphology of PC bilayers by atomic force microscopy (AFM), as well as their affinity to PC vesicles. The peptides were also analyzed structurally in PC bilayers by FTIR spectroscopy and in solution by CD spectroscopy. The results are discussed in line with gp41's role in the actual fusion process.

Results

Three peptides and their fatty acid-conjugated analogs were synthesized: N36 and N54, which are derived from gp41 ectodomain, and GCN4 coiled coil, which served as a control owing to its ability to form trimers similarly to N36 (Figure 1). Palmitic acid ($C_{16}H_{32}O_2$) and decanoic acid ($C_{10}H_{20}O_2$) were coupled to the N terminus of the peptides in order to substitute the hydrophobic FP. The peptides and their fatty acid-conjugated analogs were studied in the presence of PC model membranes, which mimic the outer zwitterionic plasma membrane and viral membrane. Since C16-N54 was active similarly to C10-N54 it was not included.

Fatty acid conjugation dramatically enhanced the fusogenic activity of the HIV-1 derived ectodomain peptides toward PC LUV

We compared the lipid mixing activity of the peptides before and after their coupling to the two fatty acids. We used as a reference the lipid mixing activity of the first 33 N terminus amino acids (FP33) which includes the 16 amino acid FP and the

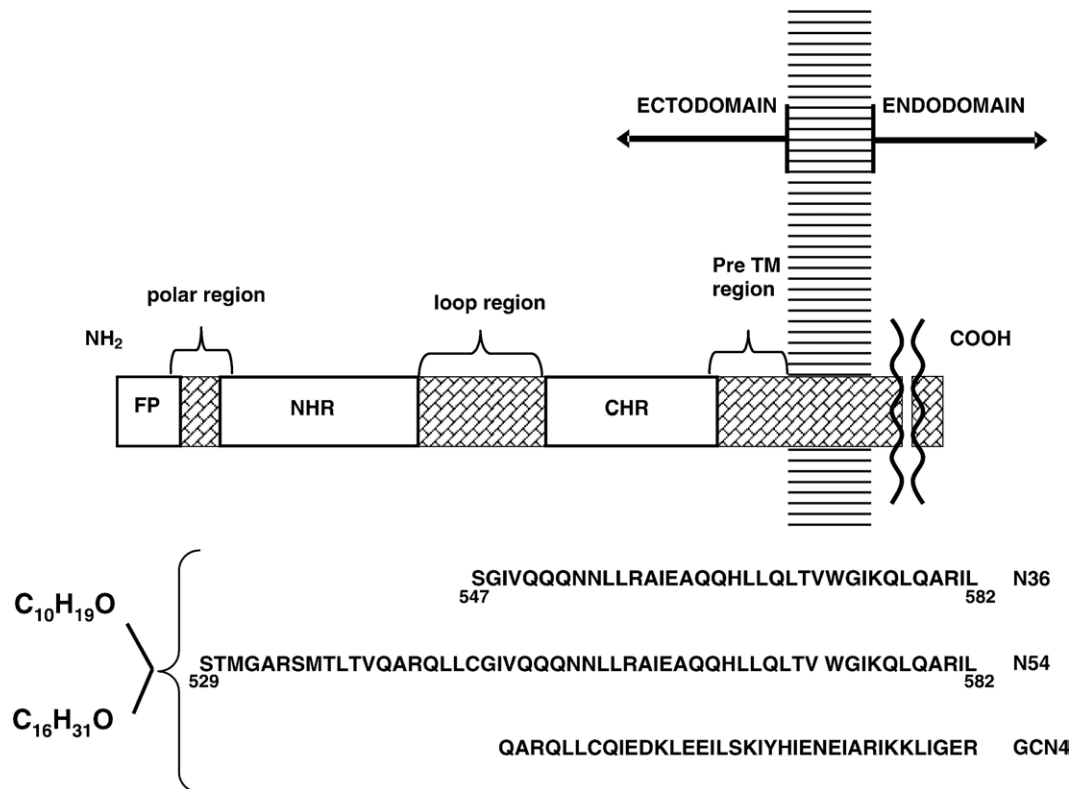


Figure 1. Scheme of the HIV primary structure. Primary functional regions are colored in white and outlined, with additionally characterized regions specified by a brace. Below the scheme are displayed the peptides represented in this study, which are derived from the N' terminal and polar region sub-domains. The residues are numbered according to their position in gp160.

adjacent polar region. The activity of this peptide is about 10% of the activity of the entire 70 N terminus (FP-N54) amino acids, which was set to 100% activity at 0.03 peptide/lipid ratio.^{28,29} The data, shown in Figure 2, reveal that N36 is inactive. However, fatty acid attachment made it very fusogenic toward PC membranes. C10-N36 and C16-N36 showed the same extent of activity at 0.07 peptide:lipid molar ratio. However, at lower peptide concentrations, C10-N36 was more active, probably due to a more intense aggregation of C16-N36. In comparison, N54 was already fusogenic before the attachment of the fatty acid. However, the attachment of decanoic acid significantly increased its fusogenic activity, especially at the lower peptide:lipid molar ratios. In contrast, the control peptide, GCN4, with the fatty acid attached, was not fusogenic either alone or after acylation. We also monitored the kinetics of the membrane fusion and the data are shown in Figure 2(b). It can be seen that the active lipopeptide acts gradually, compared with the active peptides, which have a rapid effect. The conjugated fatty acid can influence the fusion kinetics by several ways; by enhancing lipopeptides aggregation and/or by increasing membrane rigidity, which would decelerate the fusion process. Overall, the data reveal that fatty acid coupling to HIV gp41-derived peptides greatly increased their fusogenic ability. In addition, we can conclude from the results that the

fatty acid itself was not responsible for the actual fusion process, since when it was coupled to the GCN4 control peptide the newly formed lipopeptide was not fusogenic.

Visible absorbance studies supported the lipid mixing assay results

Membrane apposition is a necessary step before membrane fusion can occur. The ability of the peptides to induce vesicle aggregation was tested in order to investigate whether this property is responsible for the differences in their fusogenic activity. Changes in the vesicles' size distribution, resulting from aggregation and/or fusion, can be monitored by following the absorbance of liposome suspension. The changes in the absorbance at 405 nm as a function of time after the addition of 7 μM peptide to PC LUV suspension are shown in Figure 3. The results are in agreement with the lipid mixing assay. The attachment of fatty acids to HIV gp41-derived peptides improved their ability to induce aggregation and/or fusion of the PC LUVs.

Real-time AFM exhibited nanoscale holes in zwitterionic membranes induced by the lipopeptides

Topographic images obtained for PC bilayers in phosphate-buffered saline (PBS) reveal a single

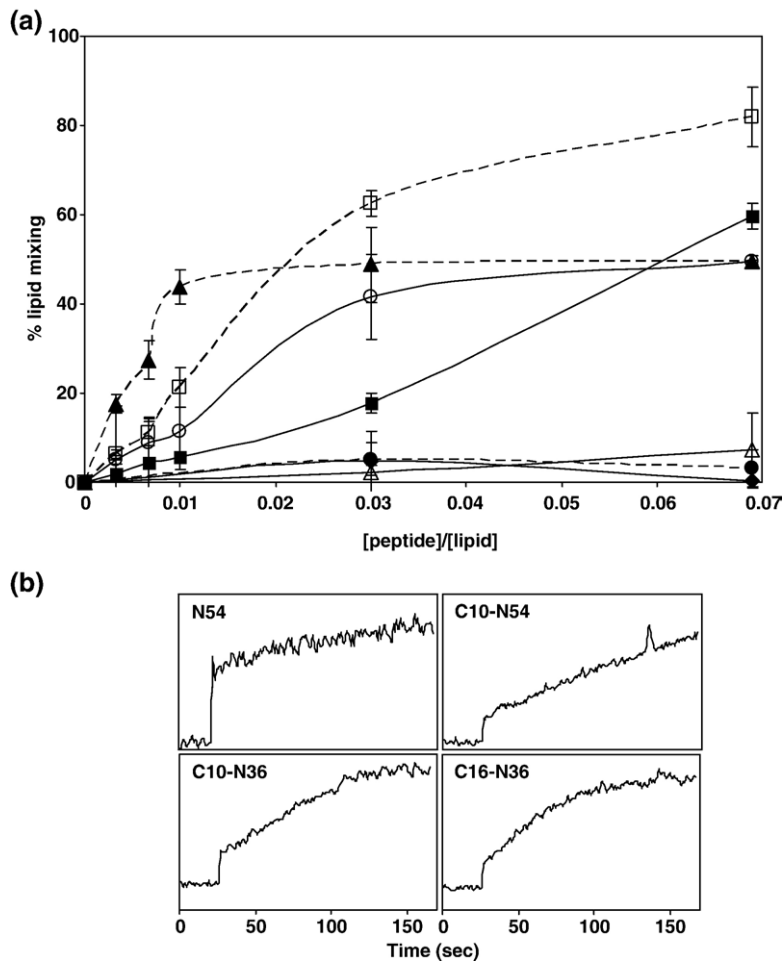


Figure 2. (a) Dose-dependent lipid mixing of PC LUV induced by the peptides and acylated peptides. Bars indicate the standard deviation of experimental measurements. Peptide aliquots were added to 100 μM PC LUV containing 10% pre-labeled LUV with 0.6 mol % NBD-PC and Rho-PC in PBS buffer. Increase of NBD-PC fluorescence intensity was measured 10 min after addition of the peptide and the percentage from the maximum (defined as ten times fluorescence intensity resolved from 0.03 peptide/lipid with FP) was plotted *versus* the peptide:lipid molar ratio. Peptide designations are as follows: C10-N54 (\square); N54 (\blacksquare); C10-N36 (\blacktriangle); C16-N36 (\circ); N36 (\blacklozenge); C10-GCN4 (\bullet); C16-GCN4 (\triangle). (b) The kinetics of the peptides and lipopeptide activity in the lipid mixing assay. The changes in the fluorescence (arbitrary units) plotted *versus* time (s), after adding peptide, are shown.

phase, continuous membrane layer, roughly 5 nm deep (data not shown). Incubation of the same bilayer region with 6 μM of C10-GCN4 (an inactive lipopeptide), or C10-N36 (an active lipopeptide) or N54 (an active peptide) in PBS was performed for approximately 5 to 10 min and new topographic images were taken every few minutes. In Figure 4, four representative pictures of each peptide are

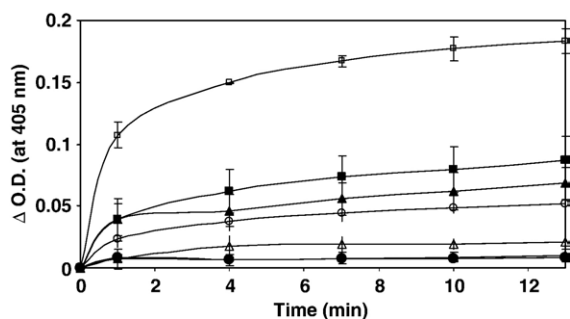


Figure 3. Fusion detection by a change in the absorbance of LUV mixed with the peptide at 405 nm. Bars indicate the standard deviation of the experimental measurements. The peptides were added to 100 μM PC LUV in PBS buffer. The changes in the absorbance are plotted *versus* the time after adding a peptide. Peptide's designations are as follows: C10-N54 (\square); N54 (\blacksquare); C10-N36 (\blacktriangle); C16-N36 (\circ); N36 (\blacklozenge); C10-GCN4 (\bullet); C16-GCN4 (\triangle).

shown. C10-GCN4, as expected, was hardly active and did not change the membrane morphology appreciably. However, both N54 and C10-N36 damaged the membrane seriously, though differently. N54, in agreement with the lipid mixing kinetic results, damaged the membrane immediately and did not induce distinctive pores, but rather had a global effect on the membrane morphology. On the other hand, C10-N36 acted gradually, as expected and created nanoholes in the phospholipid surface. Our understanding of the mechanism by which the peptides induced this morphology is still limited.

The peptides and their fatty acid-derivatives bind similarly to zwitterionic phospholipids

A decrease of tryptophan fluorescence, associated with a blue shift, was observed upon addition of PC unilamellar vesicles (SUV) to the peptide solution (Figure 5), suggesting that all three peptides bind the membrane. The reduction in the intensity of the fluorescence is probably the result of self-quenching due to the association of the peptides in the membrane upon binding. The calculated surface partition coefficient of N54 was $1.30(\pm 0.03) \times 10^4 \text{ M}^{-1}$ and that of C10-N36 was $1.70(\pm 0.01) \times 10^4 \text{ M}^{-1}$. N36, although not fusogenic, has a partition coefficient similar to that of other

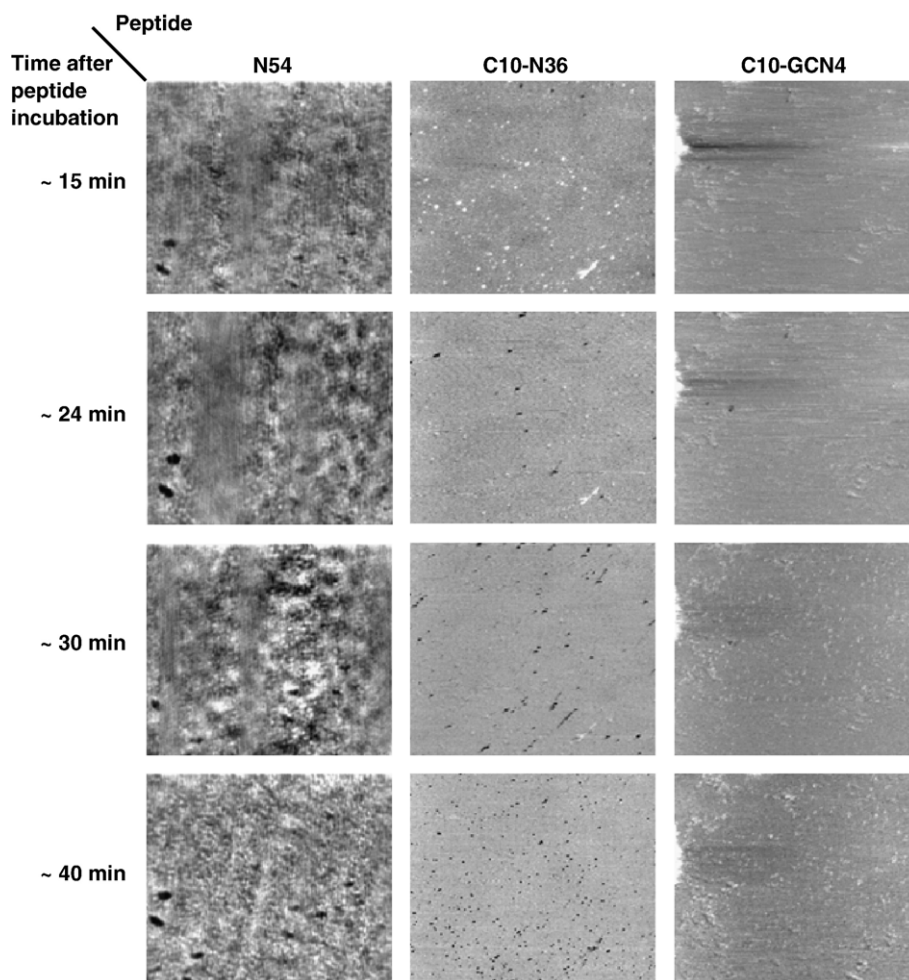


Figure 4. Real-time AFM images ($3\ \mu\text{m} \times 3\ \mu\text{m}$; z scale, 9 nm) showing the interaction between the PC bilayer membrane and N54, C10-N36, and C10-GCN4. The interactions were imaged in real time, in aqueous buffer with AFM. After 5 to 10 min incubation, new topographic images were taken every few minutes.

two fusogenic peptides ($1.10(\pm 0.40) \times 10^4\ \text{M}^{-1}$). The results suggest that the difference in the peptides' fusogenic ability is not related to their different affinity to PC membranes.

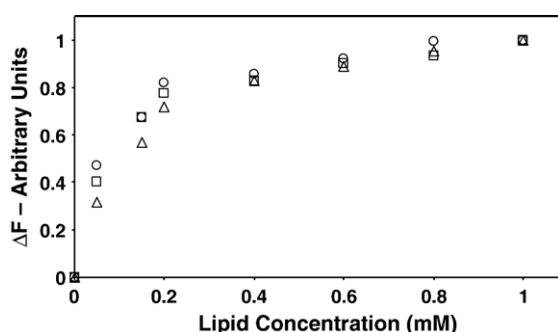


Figure 5. N54, N36, and C10-N36 bind membranes with similar affinities. Changes in the intrinsic tryptophan fluorescence intensity of N54, N36, and C10-N36 when titrated with PC SUV. K_a values derived from the charts show minor differences in the peptides' affinity toward the zwitterionic membrane. Peptide designations are as follows: N54, empty square; C10-N36, empty circle; N36, empty triangle.

The secondary structure of the free and acylated peptides in PC membranes are α -helices, as determined by using Attenuated Total Reflection Fourier Transform Infrared (ATR-FTIR) spectroscopy

We used ATR-FTIR spectroscopy to examine whether the attachment of the fatty acid to the different peptides had an effect on their secondary structure in the membrane. In the amide I region, different secondary structure components can be characterized by resolvable vibrational frequencies. In order to best resolve between helical and disordered structures that overlap, we analyzed the infra-red (IR) spectra of membrane-associated peptides following complete deuteration. The position of the component bands in the amide I spectra were identified as peaks in the second derivative. These wavelengths were used as initial parameters for curve fitting with Gaussian component peaks. The FTIR spectra for the lipopeptides and N36, which served as a positive control, together with their different component peaks, are shown in Figure 6. All lipopeptides had at least 70% α -helix content similarly to N36, which is known to adopt an α -

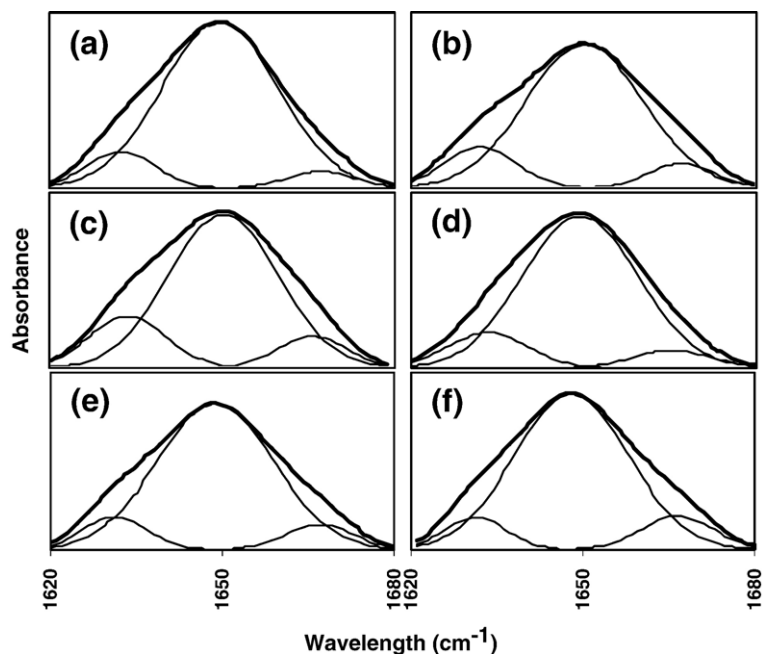


Figure 6. ATR-FTIR spectra of deuterated amide I band (1620–1680). FTIR spectra deconvolution of the fully deuterated amide I band (1620 cm^{-1} to 1680 cm^{-1}) of peptides in PC multi-bilayers. Second derivatives were calculated to identify the positions of the component bands in the spectra. The component peaks result from curve fitting using a Gaussian line shape. The sums of the fitted components superimpose on the experimental amide I region spectra. Thick lines represent the experimental FTIR spectra; thin lines represent the fitted components. Peptides C10-GCN4, C18-GCN4, N36, C10-N36, C18-N36 and C10-N54 are shown in (a–f), respectively.

helix structure in PC membranes.³⁷ These data demonstrated that fatty acid attachment did not notably change the structure of the peptide in PC membranes.

The secondary structure of the acylated peptides in solution is α -helix, as determined by using CD spectroscopy

As a corollary to the FTIR structural studies, we used CD spectroscopy to characterize the secondary structure of the free peptides and their fatty acid derivatives in solution, at low and high con-

centrations. The concentrations used for N36, N54 and their derivatives were 1 μM and 10 μM , and for GCN4 and its derivatives 1.4 μM and 14 μM . All the peptides were dissolved in 5 mM Hepes buffer. The data, shown in Figure 7, clearly demonstrate that the spectra of each peptide in 1 μM include double minima at ~ 208 nm and at ~ 222 nm, characteristic of an α -helical structure. The ellipticities of the peptides and their derivatives decreased by raising the concentration to 10 μM and also by fatty acid attachment, probably due to enhancement of the tendency of the peptides to aggregate.

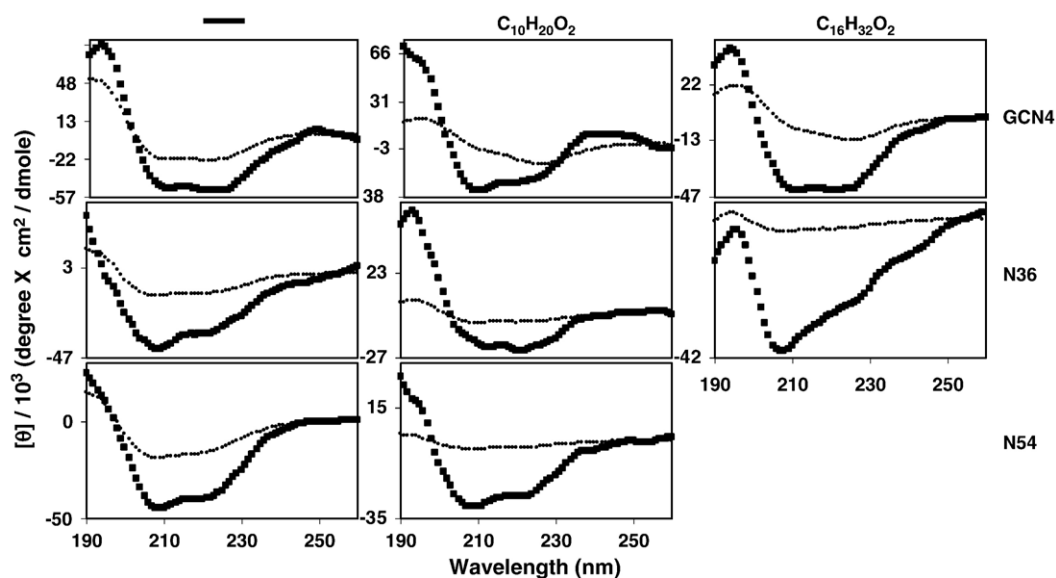


Figure 7. CD spectra of the peptides in Hepes buffer. For each peptide two different concentrations were measured: for N36, N54 and their derivatives 1 μM and 10 μM were used; and for GCN4 and its derivatives 1.4 μM and 14 μM were used. Thin lines are for the high concentrations and thick lines for the low concentration.

Discussion

Protein palmitoylation is a post-translational modification that was shown to be required for the function of a variety of fusion proteins participating in membrane fusion in various eukaryotic systems.^{22,38–40} These proteins have a highly conserved cysteine-rich domain that potentially can undergo palmitoylation, which plays an essential role in membrane targeting and anchoring.²² Such domains do not exist in viral fusion proteins, and instead, the fusion peptide is responsible for membrane association. In contrast to the cysteine-rich domain, the fusion peptide is intrinsically hydrophobic and does not require additional hydrophobic modification in order to fulfill its role.³⁶ The important finding here is that fatty acids can replace the fusion peptide, thus making the acylated NHR highly fusogenic toward zwitterionic membranes, which compose the outer leaflet of eukaryotic cells. These results imply that an analogy exists between the eukaryotic cysteine-rich domain and the viral fusion peptide, and mark the hydrophobic nature of FP as an important characteristic for its role in lipid merging.

The hydrophobic nature of the FP is a major factor in its role in lipid merging

Attachment of fatty acids to N36 and N54 significantly enhanced their fusogenic activity, as seen in the lipid mixing assay. A dramatic effect was obtained with N36, which alone cannot fuse zwitterionic membranes,¹ but turns into a very fusogenic peptide after acylation. The attached fatty acid does not significantly change the peptide's affinity to the zwitterionic membrane, as seen in the binding assay results. Apparently the fatty acid affects the peptide activity after it binds to the membrane, probably by promoting the peptide penetration into the membrane, thus mimicking the role of the fusion peptide in facilitating fusion. These results indicate that the hydrophobicity of FP, and not necessarily its specific sequence, is important for its ability to induce lipid merging. In agreement with this it has been shown that the substitution of the highly conserved phenylalanine¹¹ to valine (F11V), which presumed not to significantly affect the hydrophobicity of this region, reduced fusogenic activity by only ~50% compared to the wild-type (WT), while the substitution of the phenylalanine¹¹ to glycine abolished the fusion activity completely.¹⁸ Nevertheless, the specific sequence of the fusion peptide has also a role in membrane fusion, and in addition, it has been shown to be important for other functions, such as specific binding to the transmembrane domain of the T-cell receptor and inactivating T cells.^{41,42}

The contribution of the FP to the fusion process is reflected by our findings that C10–N54 (Figure 2(a)) is less fusogenic than FP–N54, which gives 100% activity at 0.03 peptide:lipid molar ratio,^{28,29} though,

the FP alone (N terminus 16 amino acids) is not active on PC membranes.¹⁸ In addition, when the FP is a part of a larger gp41 derived fragment, the fragment activity is sensitive to mutations within the FP, which in turn, could affect its oligomeric state. Overall, apparently the specific structure is crucial for inducing oligomerization,^{37,43} a function that can be only partially fulfilled by the hydrophobic fatty acid. Another explanation for the difference in the fusogenic activities of the lipopeptide and FP–N54 could be their different influence on membranes. While FP can increase membrane-negative curvature²⁶ and by that facilitates fusion, a saturated fatty acid will probably promote membrane rigidity which can slow down the fusion process.

The fusogenic activity of N36 and N54 supports the notion that the actual fusion process initiates before gp41 folds into SHB conformation

Since the crystal structure of the gp41 core was reported,¹² an unresolved question is what are the sequential events that take place following gp41 activation, which lead to pore formation and fusion. One possibility is that SHB formation occurs prior to pore formation, and is therefore essential for its initiation. This is based on several findings including: (i) ectodomains of many viral fusion proteins fold into bundles when in solution; (ii) peptides that block bundle formation prevent fusion^{44,45}; (iii) mutations in gp41 that abolish infectivity and fusion often map to residues within the heptad repeats that are expected to stabilize the SHB.^{44,46–49} Overall, this model suggests that the main function of NHR in the fusion process is to stabilize the trimeric oligomeric state of the gp41 ectodomain, forming a central coiled coil at the PHI stage. This conformation allows the close apposition between the viral and target cell membranes, which is crucial for increasing the ability of FP to fuse membranes. Note that all of these studies considered FP as the only region within the ectodomain of gp41, which is directly involved in membrane perturbation and fusion. However, recent accumulating data revealed that other regions within gp41 could be involved in membrane destabilization and fusion.^{1,24–33} Hence, a different possible model for gp41 fusion mechanism is that the pore-forming conformation is extended upstream of the SHB. This model is supported by several recent studies including: (i) Markosyan *et al.*,¹⁴ who used a temperature jump technique to show that pores are formed before the folding of gp41 into bundles is complete; (ii) Dimitrov *et al.*,⁵⁰ who monitored temporal conformational states of gp41 by using various monoclonal antibodies, and concluded that two parallel pathways of gp41 conformational rearrangements coexist: one leading to SHB formation and the other leading to the generation of gp41 monomers. The present findings support this notion since: (i) the attachment of fatty acids to N36, but not to the

control GCN4, turned it into an active fusogenic peptide toward zwitterionic membranes; and (ii) N54, which does not contain the fusion peptide, showed high fusogenic activity with or without the attached fatty acid.

The fusogenic conformation of N36 and N54 in zwitterionic membranes is an α -helix

FTIR results revealed an α -helical conformation in PC membranes for all the peptides and their fatty acid derivatives. This suggests that the fatty acid does not affect the activity of the peptides by changing their conformation into a more active one, but rather by anchoring them to the membrane and making it easier for the hydrophobic peptidic moiety to insert into the membrane. In addition, the data suggest that the α -helix is the fusogenic active conformation of the peptides in PC phospholipid membranes that compose most of the outer leaflet of eukaryotic cell membranes. The zwitterionic membrane is the first barrier that gp41 meets during virus–cell fusion. This is a very interesting observation, since it has been shown recently that the fusogenic active conformation of N36 in negatively charged membrane is β -sheet.¹ Importantly, the α -helical conformation of NHR in the outer leaflet does not prevent SHB formation, whereas the β -sheet conformation of NHR in the inner leaflet or in the presence of exposed negatively charged membranes cannot form SHB.¹ The insertion of FP into the target membrane cause disturbance that is likely to be sufficient for inducing transient, local exposure of electronegative phospholipids to the outer leaflet, as it has been shown that the forces acting at the contact surfaces of cell–cell^{51,52} or cell virus⁵³ interaction that lead to fusion cause exposure of phosphatidyl serine (PS). We suggest that this transient exposure of electronegative phospholipids is sufficient to trigger conformation change of NHR from α -helix to β -sheet.

In summary, the finding that fatty acids can replace the FP of HIV gp41 without loss of membrane fusion ability supports our notion of an analogy between the viral fusion peptide and the cysteine-rich domain palmitoylation of several eukaryotic fusion proteins, and mark FP's hydrophobic nature as the main characteristic that influences its function in the lipid merging process. In addition, our results show that both N54 and N36 can induce fusion, and by that means support the fusion mechanism in which the pore-forming conformation of gp41 is extended upstream of the SHB.

Materials and Methods

Materials

Rink amide-4-methylbenzhydrylamine hydrochloride salt (MBHA) resin, 4-methylbenzhydrylamine (BHA) resin, and 9-fluorenylmethoxycarbonyl (Fmoc) amino acids were obtained from Calbiochem Novabiochem

(Darmstadt, Germany). Decanoic and palmitic acid were purchased from Sigma (St. Louis, MO). Other reagents used for peptide synthesis included trifluoroacetic acid (TFA; Sigma), piperidine (Merck, Darmstadt, Germany), *N,N*-diisopropylethylamine (DIEA; Sigma), *N*-methylmorpholine (NMM; Fluka, Seelze, Germany), *N*-hydroxybenzotriazole hydrate (HOBt, Aldrich, St. Louis, MO), and 2-(1H-benzotriazol-1-yl)-1,1,3,3-tetramethyluronium hexafluorophosphate (HBTU) and dimethylformamide (DMF, peptide synthesis grade; Bio-Lab, St. Paul, MN). PC (from egg yolk), was purchased from Lipid Products (South Nutfield, U.K.). *N*-(lissamine rhodamine B sulfonyl) dioleoylphosphatidylethanolamine (Rho-PE) and *N*-(7-nitrobenz-2-oxa-1,3-diazol-4-yl) dioleoylphosphatidylethanolamine were purchased from Molecular Probes (Eugene, OR). All other reagents were of analytical grade. Buffers were prepared in double-distilled water.

Peptide synthesis, acylation, and purification

Peptides were synthesized by a 9-fluorenylmethoxycarbonyl (Fmoc) solid-phase method on Rink amide MBHA resin, by using an ABI 433A automatic peptide synthesizer. The lipophilic acid was attached to the N terminus of a resin-bound peptide by standard Fmoc chemistry, removal of the Fmoc from the N terminus of the peptide with a solution of 20% (v/v) piperidine in DMF, and fatty acid (seven equivalents, 1 M in DMF) attachment to the resin under similar conditions used for the coupling of an amino acid. The peptides were cleaved from the resin with 95% trifluoroacetic acid (TFA) and were purified by RP-HPLC on a C4 Bio-Rad semi-preparative column (250 mm \times 10 mm, 300 Å pore size, 5 μ m particle size). The purified peptides were shown to be homogeneous (>98%) by analytical RP-HPLC. Electrospray mass spectroscopy was used to confirm their molecular mass.

Preparation of unilamellar vesicles

Thin films of PC were generated following dissolution of the lipids in a 2:1 (v/v) mixture of CHCl₃/MeOH and then dried under a stream of nitrogen gas while rotating. Two populations of films were generated: (1) unlabeled, containing only PC and (2) labeled, containing PC and 0.6% molar of NBD-PE and RHO-PE each. The films were lyophilized overnight, sealed with argon gas to prevent oxidation, and stored at -20 °C. Before the experiment, the films were suspended in the appropriate buffer and vortexed for 1.5 min. The lipid suspension underwent five cycles of freezing–thawing and then extrusion through polycarbonate membranes with 1 μ m and 0.1 μ m diameter pores for 25 times to create large unilamellar vesicles (LUVs). In order to prepare the small unilamellar vesicles (SUVs), unlabeled films were dissolved in the appropriate buffer, vortexed for 1.5 min, sonicated until clear, and diluted further.

Fluorescence spectroscopy

All fluorescence measurements were performed on a SLM-AMINCO Bowman series 2-luminescence spectrometer at room temperature. Typical spectral bandwidths were 8 nm for excitation and 8 nm for emission. The sample was placed in 5 mm \times 5 mm quartz cuvettes with constant magnetic stirring. The data were corrected for background intensities and progressive dilution.

Lipid mixing assay

Lipid mixing of LUVs was measured using a fluorescence-probe dilution assay.⁵⁴ LUVs were prepared with PBS, as described above, from a mixture of unlabeled and labeled films at a 9:1 ratio of 100 μM total lipid concentration. The basal fluorescence level was measured initially for a 400 μl vesicle mixture. Then, peptide dissolved in a maximum volume of 7 μl of dimethyl sulfoxide (DMSO) was added. Fluorescence was monitored for a maximum of 15 min after addition of the peptide, to ensure a steady state, as indicated by a plateau. The emission of NBD, the energy donor, was monitored at 530 nm with the excitation set at 467 nm. Fluorescence intensity before peptide addition was referred to as 0% lipid mixing. A 100% lipid mixing was normalized according to 10×0.03 [peptide:lipid] of FP.

Visible absorbance measurements

Changes in the size of vesicles were measured by visible absorbance. Aliquots of peptide stock solutions were added to 400 μl suspensions of 100 μM PC LUV in PBS. The absorbance at 405 nm was monitored with time using a Bio-Tek Instrument microplate reader before and after the addition of peptide.

Preparation of supported lipid bilayers

Supported lipid bilayers were prepared using the vesicle fusion method.⁵⁵ Briefly, PC LUV suspensions (0.7 mM, 70 μl) were deposited onto freshly cleaved mica squares (1 cm^2) and allowed to adsorb and fuse on the solid surface for 12 h at 4 $^\circ\text{C}$. Samples were then placed in a 1.1 ml liquid chamber for AFM measurements. The band positions were determined after smoothing the spectra by applying the methods by Savitzky-Golay.

Atomic force microscopy (AFM)

Supported bilayers were investigated using a commercial atomic force microscope (NTEGRA, NT-MDT, Zelenograd, Russia) equipped with a 100 $\mu\text{m} \times 100 \mu\text{m} \times 5 \mu\text{m}$ Smena scanner. AFM images were obtained in semi-contact mode at room temperature (23–25 $^\circ\text{C}$) in a 1.1 ml liquid cell (MP1LC) filled with either PBS buffer containing ~3.5% DMSO. The peptides were dissolved in DMSO and diluted in 30 mM NaCl to ~3.5% DMSO. Next, they were injected into the liquid chamber to reach a 6 μM peptide concentration, and images were taken continuously every ~3 min. All images were recorded using oxide-sharpened micro-fabricated Si_3N_4 cantilevers (DNP-S; Veeco Metrology LLC, Santa Barbara, CA) with a spring constant of ~0.3 N/m (manufacturer specified) and at a scan rate of 1–1.5 Hz. Large scale images were taken after each scan to ensure that changes in membrane morphology were not caused by the tip.

Membrane binding

N54, N36, and C10–N36 interactions with membranes were analyzed and quantified using fluorescence anisotropy of their intrinsic Trp residue in the presence of PC phospholipid model membranes. Excitation and emission wavelengths were set to 280/350 nm, respectively, and 1 μM of peptide (in 400 μl of PBS) was titrated with

13.3 mM membrane solution successively. Since Trp is known to change its emission in a hydrophobic environment,⁵⁶ a change in its emission represented the amount of peptide bound to membranes. The system reached binding equilibrium (F_{max}) at a certain lipid/peptide ratio, allowing us to calculate the affinity constant from the relations between the equilibrium level of Trp emission and the lipid concentration (C), using a steady-state affinity model. The affinity constants were then determined by non-linear least-squares (NLLSQ). The NLLSQ fitting was done using the following equation:

$$Y(x) = \frac{K_a \times X \times F_{\text{max}}}{1 + K_a \times X}$$

where X is the lipid concentration, Y(x) is the fluorescence emission, F_{max} is the maximal difference in the emission of Trp-containing peptide before and after the addition of lipids (it represents the maximum peptide bound to lipid), and K_a is the affinity constant.

Attenuated total reflection FTIR Spectroscopy

Spectra were obtained with a Bruker equinox 55 FTIR spectrometer equipped with a deuterated triglyceride sulfate (DTGS) detector and coupled with an ATR device. For each spectrum, 250 scans were collected with a resolution of 4 cm^{-1} . Samples were prepared as described.⁵⁷ Briefly, lipids alone or with peptide were deposited on a ZnSe horizontal ATR prism (80 mm \times 7 mm). Before sample preparation, the trifluoroacetate (CF_3COO^-) counterions, which associate strongly with the peptide, were replaced with chloride ions through several washings in 0.1 M HCl and lyophilization. This eliminated the strong C=O stretching absorption band near 1673 cm^{-1} .⁵⁷ Peptides were dissolved in MeOH and lipid films in a 1:2 (v/v) MeOH/ CHCl_3 mixture. Lipid/peptide mixtures or lipids alone with the corresponding volume of methanol were spread with a Teflon bar on the ZnSe prism. Solvents were eliminated by drying under vacuum for 15 min. The background for each spectrum was a clean ZnSe prism. Samples were hydrated by introducing an excess of deuterium oxide ($^2\text{H}_2\text{O}$) into a chamber placed on top of the ZnSe prism in the ATR casting and incubated for up to 60 min, with spectra acquisition every five to 10 min. Hydrogen/deuterium exchange was considered complete due to the complete shift of the amide II band. Subtraction of atmospheric H_2O vapor for each sample was carried out as described.⁵⁸ The absorbance of peptide(s) alone was obtained by subtracting the signal of the peptides in lipid from lipid alone (for H_2O -corrected spectra), each deuterated for an equal time. We processed the subtracted spectra using PEAKFIT (Jandel Scientific, San Rafael, CA) software. For an accurate comparison, the absorption of the peptide(s) alone in amide I (1620–1680 cm^{-1}) was baseline-corrected. Second-derivative spectra were calculated to identify the positions of the component absorption peaks in the spectra.

Circular dichroism

The CD spectra of the peptides were measured in an Aviv 202 spectropolarimeter. The spectra were scanned with a thermostated quartz optical cell with a path length of 1 mm. Each spectrum was recorded at 1 nm intervals with an average time of 10 s, at a wavelength range of 260 nm–190 nm. The peptides were scanned at a 10 μM or

1 μM concentration in 5 mM Hepes buffer. The α -helical content was estimated from the CD signal by dividing the mean residue ellipticity at 222 nm by the value expected for 100% helix formation ($-37,000 \text{ deg. cm}^2 \text{ dmol}^{-1}$).⁵⁹

Acknowledgements

This study was supported by the Israel Science Foundation. Y.S is the incumbent of the Harold S. and Harriet B. Brady Professorial Chair in Cancer Research. We extend our gratitude to Dr. Yishay Feldman for his assistance in the AFM experiments and data analysis and Dr. Kelly Sackett for his help throughout the study.

References

- Korazim, O., Sackett, K. & Shai, Y. (2006). Functional and structural characterization of HIV-1 gp41 ectodomain regions in phospholipid membranes suggests that the fusion-active conformation is extended. *J. Mol. Biol.* **364**, 1103–1117.
- Veronese, F. D., DeVico, A. L., Copeland, T. D., Oroszlan, S., Gallo, R. C. & Sarngadharan, M. G. (1985). Characterization of gp41 as the transmembrane protein coded by the HTLV-III/LAV envelope gene. *Science*, **229**, 1402–1405.
- Center, R. J., Leapman, R. D., Lebowitz, J., Arthur, L. O., Earl, P. L. & Moss, B. (2002). Oligomeric structure of the human immunodeficiency virus type 1 envelope protein on the virion surface. *J. Virol.* **76**, 7863–7867.
- Rabenstein, M. & Shin, Y. K. (1995). A peptide from the heptad repeat of human immunodeficiency virus gp41 shows both membrane binding and coiled-coil formation. *Biochemistry*, **34**, 13390–13397.
- Backer, J. M. & Dawidowicz, E. A. (1987). Reconstitution of a phospholipid flippase from rat liver microsomes. *Nature*, **327**, 341–343.
- Kowalski, M., Potz, J., Basiripour, L., Dorfman, T., Goh, W. C., Terwilliger, E. et al. (1987). Functional regions of the envelope glycoprotein of human immunodeficiency virus type 1. *Science*, **237**, 1351–1355.
- Martin, I., Schaal, H., Scheid, A. & Ruyschaert, J. M. (1996). Lipid membrane fusion induced by the human immunodeficiency virus type 1 gp41 N-terminal extremity is determined by its orientation in the lipid bilayer. *J. Virol.* **70**, 298–304.
- Jones, P. L., Korte, T. & Blumenthal, R. (1998). Conformational changes in cell surface HIV-1 envelope glycoproteins are triggered by cooperation between cell surface CD4 and co-receptors. *J. Biol. Chem.* **273**, 404–409.
- Melikyan, G. B., Egelhofer, M. & von Laer, D. (2006). Membrane-anchored inhibitory peptides capture human immunodeficiency virus type 1 gp41 conformations that engage the target membrane prior to fusion. *J. Virol.* **80**, 3249–3258.
- Furuta, R. A., Wild, C. T., Weng, Y. & Weiss, C. D. (1998). Capture of an early fusion-active conformation of HIV-1 gp41. *Nature Struct. Biol.* **5**, 276–279.
- Munoz-Barroso, I., Durell, S., Sakaguchi, K., Appella, E. & Blumenthal, R. (1998). Dilation of the human immunodeficiency virus-1 envelope glycoprotein fusion pore revealed by the inhibitory action of a synthetic peptide from gp41. *J. Cell. Biol.* **140**, 315–323.
- Chan, D. C., Fass, D., Berger, J. M. & Kim, P. S. (1997). Core structure of gp41 from the HIV envelope glycoprotein. *Cell*, **89**, 263–273.
- Weissenhorn, W., Dessen, A., Harrison, S. C., Skehel, J. J. & Wiley, D. C. (1997). Atomic structure of the ectodomain from HIV-1 gp41. *Nature*, **387**, 426–430.
- Markosyan, R. M., Cohen, F. S. & Melikyan, G. B. (2003). HIV-1 envelope proteins complete their folding into six-helix bundles immediately after fusion pore formation. *Mol. Biol. Cell.* **14**, 926–938.
- Schaal, H., Klein, M., Gehrman, P., Adams, O. & Scheid, A. (1995). Requirement of N-terminal amino acid residues of gp41 for human immunodeficiency virus type 1-mediated cell fusion. *J. Virol.* **69**, 3308–3314.
- Freed, E. O., Delwart, E. L., Buchsacher, G. L., Jr & Panganiban, A. T. (1992). A mutation in the human immunodeficiency virus type 1 transmembrane glycoprotein gp41 dominantly interferes with fusion and infectivity. *Proc. Natl Acad. Sci. USA*, **89**, 70–74.
- Delahunty, M. D., Rhee, I., Freed, E. O. & Bonifacino, J. S. (1996). Mutational analysis of the fusion peptide of the human immunodeficiency virus type 1: identification of critical glycine residues. *Virology*, **218**, 94–102.
- Pritsker, M., Rucker, J., Hoffman, T. L., Doms, R. W. & Shai, Y. (1999). Effect of nonpolar substitutions of the conserved Phe11 in the fusion peptide of HIV-1 gp41 on its function, structure, and organization in membranes. *Biochemistry*, **38**, 11359–11371.
- Dimitrov, A. S., Rawat, S. S., Jiang, S. & Blumenthal, R. (2003). Role of the fusion peptide and membrane-proximal domain in HIV-1 envelope glycoprotein-mediated membrane fusion. *Biochemistry*, **42**, 14150–14158.
- Durell, S. R., Martin, I., Ruyschaert, J. M., Shai, Y. & Blumenthal, R. (1997). What studies of fusion peptides tell us about viral envelope glycoprotein-mediated membrane fusion (review). *Mol. Membr. Biol.* **14**, 97–112.
- Tamm, L. K. & Han, X. (2000). Viral fusion peptides: a tool set to disrupt and connect biological membranes. *Biosci. Rep.* **20**, 501–518.
- Pallavi, B. & Nagaraj, R. (2003). Palmitoylated peptides from the cysteine-rich domain of SNAP-23 cause membrane fusion depending on peptide length, position of cysteines, and extent of palmitoylation. *J. Biol. Chem.* **278**, 12737–12744.
- Veit, M., Laage, R., Dietrich, L., Wang, L. & Ungermann, C. (2001). Vac8p release from the SNARE complex and its palmitoylation are coupled and essential for vacuole fusion. *EMBO J.* **20**, 3145–3155.
- Salzwedel, K., West, J. T. & Hunter, E. (1999). A conserved tryptophan-rich motif in the membrane-proximal region of the human immunodeficiency virus type 1 gp41 ectodomain is important for Env-mediated fusion and virus infectivity. *J. Virol.* **73**, 2469–2480.
- Munoz-Barroso, I., Salzwedel, K., Hunter, E. & Blumenthal, R. (1999). Role of the membrane-proximal domain in the initial stages of human immunodeficiency virus type 1 envelope glycoprotein-mediated membrane fusion. *J. Virol.* **73**, 6089–6092.
- Peisajovich, S. G., Epand, R. F., Pritsker, M., Shai, Y. & Epand, R. M. (2000). The polar region consecutive to the HIV fusion peptide participates in membrane fusion. *Biochemistry*, **39**, 1826–1833.

27. Suarez, T., Gallaher, W. R., Agirre, A., Goni, F. M. & Nieva, J. L. (2000). Membrane interface-interacting sequences within the ectodomain of the human immunodeficiency virus type 1 envelope glycoprotein: putative role during viral fusion. *J. Virol.* **74**, 8038–8047.
28. Sackett, K. & Shai, Y. (2002). The HIV-1 gp41 N-terminal heptad repeat plays an essential role in membrane fusion. *Biochemistry*, **41**, 4678–4685.
29. Wexler-Cohen, Y., Sackett, K. & Shai, Y. (2005). The role of the N-terminal heptad repeat of HIV-1 in the actual lipid mixing step as revealed by its substitution with distant coiled coils. *Biochemistry*, **44**, 5853–5856.
30. Pascual, R., Moreno, M. R. & Villalain, J. (2005). A peptide pertaining to the loop segment of human immunodeficiency virus gp41 binds and interacts with model biomembranes: implications for the fusion mechanism. *J. Virol.* **79**, 5142–5152.
31. Pascual, R., Contreras, M., Fedorov, A., Prieto, M. & Villalain, J. (2005). Interaction of a peptide derived from the N-heptad repeat region of gp41 Env ectodomain with model membranes. Modulation of phospholipid phase behavior. *Biochemistry*, **44**, 14275–14288.
32. Moreno, M. R., Giudici, M. & Villalain, J. (2006). The membranotropic regions of the endo and ecto domains of HIV gp41 envelope glycoprotein. *Biochim. Biophys. Acta*, **1758**, 111–123.
33. Kliger, Y., Peisajovich, S. G., Blumenthal, R. & Shai, Y. (2000). Membrane-induced conformational change during the activation of HIV-1 gp41. *J. Mol. Biol.* **301**, 905–914.
34. Epand, R. F., Macosko, J. C., Russell, C. J., Shin, Y. K. & Epand, R. M. (1999). The ectodomain of HA2 of influenza virus promotes rapid pH dependent membrane fusion. *J. Mol. Biol.* **286**, 489–503.
35. Ghosh, J. K. & Shai, Y. (1999). Direct evidence that the N-terminal heptad repeat of Sendai virus fusion protein participates in membrane fusion. *J. Mol. Biol.* **292**, 531–546.
36. White, J. M. (1990). Viral and cellular membrane fusion proteins. *Annu. Rev. Physiol.* **52**, 675–697.
37. Sackett, K. & Shai, Y. (2005). The HIV fusion peptide adopts intermolecular parallel beta-sheet structure in membranes when stabilized by the adjacent N-terminal heptad repeat: a ¹³C FTIR study. *J. Mol. Biol.* **350**, 790–805.
38. Glick, B. S. & Rothman, J. E. (1987). Possible role for fatty acyl-coenzyme A in intracellular protein transport. *Nature*, **326**, 309–312.
39. Pfanner, N., Glick, B. S., Arden, S. R. & Rothman, J. E. (1990). Fatty acylation promotes fusion of transport vesicles with Golgi cisternae. *J. Cell Biol.* **110**, 955–961.
40. Sakai, T., Ohuchi, R. & Ohuchi, M. (2002). Fatty acids on the A/USSR/77 influenza virus hemagglutinin facilitate the transition from hemifusion to fusion pore formation. *J. Virol.* **76**, 4603–4611.
41. Quintana, F. J., Gerber, D., Kent, S. C., Cohen, I. R. & Shai, Y. (2005). HIV-1 fusion peptide targets the TCR and inhibits antigen-specific T cell activation. *J. Clin. Invest.* **115**, 2149–2158.
42. Bloch, I., Quintana, F. J., Gerber, D., Cohen, T., Cohen, I. R. & Shai, Y. (2007). T-cell inactivation and immunosuppressive activity induced by HIV gp41 via novel interacting motif. *FASEB J.* **21**, 393–401.
43. Sackett, K. & Shai, Y. (2003). How structure correlates to function for membrane associated HIV-1 gp41 constructs corresponding to the N-terminal half of the ectodomain. *J. Mol. Biol.* **333**, 47–58.
44. Wild, C., Dubay, J. W., Greenwell, T., Baird, T., Jr, Oas, T. G., McDanal, C. *et al.* (1994). Propensity for a leucine zipper-like domain of human immunodeficiency virus type 1 gp41 to form oligomers correlates with a role in virus-induced fusion rather than assembly of the glycoprotein complex. *Proc. Natl Acad. Sci. USA*, **91**, 12676–12680.
45. Jiang, S., Lin, K., Strick, N. & Neurath, A. R. (1993). HIV-1 inhibition by a peptide. *Nature*, **365**, 113.
46. Dubay, J. W., Roberts, S. J., Brody, B. & Hunter, E. (1992). Mutations in the leucine zipper of the human immunodeficiency virus type 1 transmembrane glycoprotein affect fusion and infectivity. *J. Virol.* **66**, 4748–4756.
47. Pombourios, P., Wilson, K. A., Center, R. J., El Ahmar, W. & Kemp, B. E. (1997). Human immunodeficiency virus type 1 envelope glycoprotein oligomerization requires the gp41 amphipathic alpha-helical/leucine zipper-like sequence. *J. Virol.* **71**, 2041–2049.
48. Chen, S. S., Lee, C. N., Lee, W. R., McIntosh, K. & Lee, T. H. (1993). Mutational analysis of the leucine zipper-like motif of the human immunodeficiency virus type 1 envelope transmembrane glycoprotein. *J. Virol.* **67**, 3615–3619.
49. Chen, S. S. (1994). Functional role of the zipper motif region of human immunodeficiency virus type 1 transmembrane protein gp41. *J. Virol.* **68**, 2002–2010.
50. Dimitrov, A. S., Louis, J. M., Bewley, C. A., Clore, G. M. & Blumenthal, R. (2005). Conformational changes in HIV-1 gp41 in the course of HIV-1 envelope glycoprotein-mediated fusion and inactivation. *Biochemistry*, **44**, 12471–12479.
51. Driesen, R. B., Dispersyn, G. D., Verheyen, F. K., van den Eijnde, S. M., Hofstra, L., Thone, F. *et al.* (2005). Partial cell fusion: a newly recognized type of communication between dedifferentiating cardiomyocytes and fibroblasts. *Cardiovasc. Res.* **68**, 37–46.
52. Van den Eijnde, S. M., Van den Hoff, M. J., Reutelingsperger, C. P., Van Heerde, W. L., Henfling, M. E., Vermeij-Keers, C. *et al.* (2001). Transient expression of phosphatidylserine at cell-cell contact areas is required for myotube formation. *J. Cell Sci.* **114**, 3631–3642.
53. Gautier, I., Coppey, J. & Durieux, C. (2003). Early apoptosis-related changes triggered by HSV-1 in individual neuronlike cells. *Exp. Cell Res.* **289**, 174–183.
54. Struck, D. K., Hoekstra, D. & Pagano, R. E. (1981). Use of resonance energy transfer to monitor membrane fusion. *Biochemistry*, **20**, 4093–4099.
55. Yang, T., Simanek, E. E. & Cremer, P. (2000). Creating addressable aqueous microcompartments above solid supported phospholipid bilayers using lithographically patterned poly(dimethylsiloxane) molds. *Anal. Chem.* **72**, 2587–2589.
56. Jameson, D. M. & Sawyer, W. H. (1995). Fluorescence anisotropy applied to biomolecular interactions. *Methods Enzymol.* **246**, 283–300.
57. Surewicz, W. K., Mantsch, H. H. & Chapman, D. (1993). Determination of protein secondary structure by Fourier transform infrared spectroscopy: a critical assessment. *Biochemistry*, **32**, 389–394.
58. Vigano, C., Goormaghtigh, E. & Ruysschaert, J. M. (2003). Detection of structural and functional asymmetries in P-glycoprotein by combining mutagenesis and H/D exchange measurements. *Chem. Phys. Lipids*, **122**, 121–135.
59. Wu, C. S., Ikeda, K. & Yang, J. T. (1981). Ordered conformation of polypeptides and proteins in acidic dodecyl sulfate solution. *Biochemistry*, **20**, 566–570.